Dynamical mean field theory study of a simplified model for CuO_2 planes

2005 J. Phys.: Condens. Matter 17 8079

(http://iopscience.iop.org/0953-8984/17/50/025)

INSTITUTE OF PHYSICS PUBLISHING JOURNAL OF PHYSICS: CONDENSED MATTER

J. Phys.: Condens. Matter **17** (2005) 8079–8089 doi:10.1088/0953-8984/17/50/025

Dynamical mean field theory study of a simplified model for CuO_2 planes

A Beatrici[1,2] **and M A Gusmão**[1]

[1] Instituto de Física, Universidade Federal do Rio Grande do Sul, CP 15051, 91501-970 Porto Alegre, RS, Brazil
[2] Departamento de Física, Centro Universitário La Salle, 92010-000 Canoas, RS, Brazil

Received 15 September 2005
Published 2 December 2005
Online at stacks.iop.org/JPhysCM/17/8079

Abstract

Following previous work on Hubbard and Anderson models, we introduce a simplified three-band Hubbard model for CuO_2 planes of high-T_c superconductors. This allows for exact evaluation of single-particle Green's functions within the dynamical mean field approach. Keeping information about the lattice structure through the appropriate bare density of states, we study the existence of magnetic solutions, and their stability with respect to variations of the doping fraction, interaction parameters, and temperature. Normal-state properties of known superconducting cuprates are reproduced, and we show that the model has room for substantial enhancement of Néel temperatures.

1. Introduction

For almost two decades now a great deal of experimental and theoretical effort has been devoted to studying interesting properties of the so called high-T_c superconductors (HTSCs), discovered by Bednorz and Müller [1] in 1986. Currently, the HTSCs include many families of cuprates, such as $La_{2-x}(Ba, Sr)_xCuO_{4+y}$, $YBa_2Cu_3O_{6+y}$, $Bi_2Sr_2CaCu_2O_{8+y}$, $Tl_2Ba_2CuO_{6+y}$, $Nd_{2-x}Ce_xCuO_4$, etc. These compounds present properties so diverse from conventional superconductors that they cannot fit into the BCS scheme [2], at least with respect to the coupling mechanism. Experimentally, their behaviour has been well determined, both in the normal and superconducting states [3–5]. From the theoretical point of view, however, successful results are still very limited. For instance, studies of the superconducting state have not in general dealt with truly microscopic models. The only consensus refers to the importance of CuO_2 planar structures that are common to all of these systems. Electronic correlations on the CuO_2 planes can account for the observed magnetic properties of undoped compounds, and holes or electrons doped into these planes are responsible for the transport properties, which implies that they are certainly involved in the establishment of superconductivity.

It is widely accepted that a single-band effective Hubbard model is well suited to describe the relevant physics of these CuO_2 planes, after the pioneering work by Zhang and Rice [6].

Nevertheless, if one wants to study the interplay between Coulomb correlation and inter-band charge transfer, the basic model to be employed is the so-called three-band Hubbard model [7], which includes both charge-transfer effects due to hybridization of copper 3d and oxygen 2p orbitals, and strong-correlation effects due to Coulomb repulsion on the copper sites. Obviously, this defines a complex many-body problem, whose study must rely on suitable approximation methods. Leaving aside simple mean-field theories, and given that methods related to the Hubbard I approximation [8] yield changes to the expected nature of the magnetically ordered state of this model [9], it is natural to look for some kind of perturbation approach using Matsubara Green's functions, as we are interested in finite-temperature properties. However, the strongly correlated nature of the problem precludes utilization of standard many-body techniques, while strong-coupling methods tend to be much less systematic.

This research field received a new impetus with the introduction of the dynamical mean field theory (DMFT) [10], which maps the lattice problem to a single-site problem in the presence of a self-consistent dynamical mean field accounting for the effect of the surrounding lattice. Although this mapping is exact only in infinite spatial dimensions, the method proved to be a good approximation for finite dimensions. Apart from the dimensionality issue, one should bear in mind that the effective one-site problem dealt with in DMFT is highly non-trivial, and in general cannot be solved exactly. Early studies of the one-band Hubbard model or the periodic Anderson model (PAM) have resorted to quantum Monte Carlo, iterated perturbation theory (IPT) and/or the non-crossing approximation [10]. These methods tend to be computationally demanding, and present strong applicability constraints. On the other hand, a simplified version of the Hubbard model was proposed [11, 12] in which electrons with a given spin orientation are *frozen* when determining the spectral properties of electrons with opposite spin. This amounts to neglecting spin-flip processes when evaluating on-site correlations, and can be shown to map into the Falicov–Kimball (FK) model [13]. Its main interest lies in the fact that it can be *exactly solved* in infinite dimensions [14, 15]. A similar simplification was applied to the PAM, also allowing for an exact solution through the DMFT approach [16].

In the present paper, we extend this idea, introducing a simplified three-band Hubbard model to study the electronic structure and magnetic properties of high-T_c superconductors in their normal state. Previous results for the one-band Hubbard model [17] showed that spin-flip processes are less important for large Coulomb repulsion. This is actually the case for HTSCs, where the Mott gap of the copper d band is large, and the relevant physics is related to charge-transfer excitations between copper and oxygen levels. Thus, it is reasonable to expect that neglecting the copper-site spin-flip processes in our simplified model is not crucial, and it allows for exact evaluation of Green's functions within the DMFT approach. We, then, focus on keeping the appropriate two-dimensional uncorrelated band structure for the CuO_2 planes, and determining magnetic phase diagrams with respect to both doping and the model coupling constants.

Our results are in qualitative agreement with the observed magnetic properties, and even quantitatively good as far the Néel temperature is concerned. In addition, we were able to explore a wide region of the parameter space, showing that the model can yield substantially enhanced values of this temperature, for suitable choices of the relevant coupling constants. It is still an open question whether appropriate choices can be experimentally realized, and what changes would correspondingly occur in the superconducting properties.

This paper is organized as follows. In section 2, we discuss the relevant interactions, introducing the model Hamiltonian for CuO_2 layers, and its simplified version. In section 3, we review the DMFT approach for the single-band case. The method is then applied to the

three-band model in section 4, and its main results discussed in section 5. Final discussions and conclusions appear in section 6.

2. Interactions and Hamiltonian

Models of the HTSC are generally built upon selected fundamental interactions in the CuO_2 layers, with the remaining components of the system acting as a source of electrons or holes to this two-dimensional (2D) lattice. It is generally accepted that the physics is dominated by Coulomb correlations at the copper sites, and by copper–oxygen hybridization (hopping). Less important, and often neglected, are a direct oxygen–oxygen hopping, Coulomb repulsion at the oxygen sites, inter-site Coulomb interactions, and deviations from the square-lattice symmetry due to orthorhombic distortions.

Undoped compounds show almost full copper 3d and oxygen 2p levels, except for a single hole per CuO_2 unit. This hole resides predominantly on the copper site, yielding its magnetic character. Taking into account all level splittings due to the crystal-field symmetry [18], there is a single lowest-lying hole level of $d_{x^2-y^2}$ symmetry, followed by degenerate $p_{x,y}$ levels. Hybridization occurs between d orbitals and either p_x or p_y along the corresponding directions in the xy plane. One of the orthogonal combinations of these p orbitals gives rise to a zero-width (non-hybridized) p band. The remaining two bands, keeping only the most important contributions referred to in the previous paragraph, may be described by the following Hamiltonian (in hole representation):

$$H = -t \sum_{\langle ij\rangle\sigma} (d^\dagger_{i\sigma} p_{j\sigma} + p^\dagger_{j\sigma} d_{i\sigma}) - \Delta \sum_{i\sigma} n^{\mathrm{d}}_{i\sigma} + U \sum_i n^{\mathrm{d}}_{i\uparrow} n^{\mathrm{d}}_{i\downarrow}, \tag{1}$$

where t is the hopping constant (hybridization), i and j refer to copper and oxygen sites, respectively, $\sigma = \uparrow, \downarrow$ indicates the spin state, U stands for the Coulomb correlation, Δ is the energy difference between p and d levels (bare charge-transfer gap), and we have chosen the bare p level as the energy zero.

We now introduce the simplified Hamiltonian mentioned in section 1, which we will call H_{S}. Since the dynamics of holes with opposite spins will be decoupled, we drop the spin index, referring to, e.g, the spin-up holes on copper orbitals as d holes, while the *frozen* (spin-down) ones will be described by new spinless-fermion operators f_i and $f_i^\dagger$, with the number operator $n^{\mathrm{f}}_i = f^\dagger_i f_i$. The Hamiltonian, then, reads

$$H_{\mathrm{S}} = -t \sum_{\langle ij\rangle} (d^\dagger_i p_j + p^\dagger_j d_i) - \Delta \sum_i n^{\mathrm{d}}_i + E_{\mathrm{f}} \sum_i n^{\mathrm{f}}_i + U \sum_i n^{\mathrm{d}}_i n^{\mathrm{f}}_i. \tag{2}$$

E_{f} plays the role of a Lagrange multiplier, allowing us to fix the appropriate number of f holes.

3. DMFT—revising the one-band problem

As we mentioned before, the one-band simplified Hubbard model (FK model) has an exact solution in the context of DMFT. Since we will now generalize this approach to the two-band model of (2), we begin by quickly revising the main results of the single-band solution. The FK Hamiltonian reads

$$H_{\mathrm{FK}} = -\sum_{ij} t_{ij} d^\dagger_i d_j + U \sum_i n^{\mathrm{d}}_i n^{\mathrm{f}}_i + E_{\mathrm{f}} \sum_i n^{\mathrm{f}}_i. \tag{3}$$

The one-particle finite-temperature Green's function in the paramagnetic state can be written in the general form

$$G^{\mathrm{d}}_{\mathbf{k}}(\omega_n) = \frac{1}{\mathrm{i}\omega_n - \varepsilon_{\mathbf{k}} - \Sigma(\mathbf{k}, \omega_n) + \mu}, \tag{4}$$

in terms of the self-energy $\Sigma(\mathbf{k}, \omega_n)$, where the Matsubara frequencies are determined by the temperature T through $\omega_n = (2n+1)\pi T$, for integer n, and μ is the chemical potential. In DMFT, the lattice problem is replaced by a single-site problem with hybridization to a particle bath that accounts for the effect of the surrounding lattice. Thus, the on-site Green's function takes the form

$$G^{\mathrm{d}}_{ii}(\omega_n) = \frac{1}{\mathrm{i}\omega_n - \Sigma(\omega_n) - \mathcal{A}(\omega_n) + \mu}, \tag{5}$$

where $\Sigma(\omega_n)$ is a local self-energy accounting for the on-site interactions, and $\mathcal{A}(\omega_n)$ is the mean-field or hybridization function. Since in infinite dimensions (and, hence, in DMFT) the lattice self-energy becomes purely local [11], we can equate the self-energies appearing in (4) and (5). Even though this becomes an approximation at finite dimensions, it is recognized [10] to give good results for $d > 1$, and can be viewed as a kind of $\mathbf{k}$-space averaging of the self-energy [19]. Assuming that the on-site Green's functions calculated from the lattice or from the effective problem must be equal, we obtain the self-consistency relation

$$G^{\mathrm{d}}_{ii}(\omega_n) = \frac{1}{N}\sum_{\mathbf{k}} \frac{1}{[G^{\mathrm{d}}_{ii}(\omega_n)]^{-1} + \mathcal{A}(\omega_n) - \varepsilon_{\mathbf{k}}}, \tag{6}$$

where N is the number of lattice sites. The sum in $\mathbf{k}$ space can be replaced by an energy integration,

$$G^{\mathrm{d}}_{ii}(\omega_n) = \int \frac{\rho_0(\varepsilon)\,\mathrm{d}\varepsilon}{[G^{\mathrm{d}}_{ii}(\omega_n)]^{-1} + \mathcal{A}(\omega_n) - \varepsilon}, \tag{7}$$

$\rho_0(\varepsilon)$ being the noninteracting density of states.

We still need to solve the effective single-site problem in order to obtain another relation between G^{d}_{ii} and $\mathcal{A}$. This is easily done for the FK model, yielding

$$G^{\mathrm{d}}_{ii}(\omega_n) = \frac{1 - \langle n_{\mathrm{f}}\rangle}{\mathrm{i}\omega_n + \mu - \mathcal{A}(\omega_n)} + \frac{\langle n_{\mathrm{f}}\rangle}{\mathrm{i}\omega_n + \mu - U - \mathcal{A}(\omega_n)}. \tag{8}$$

Finally, the set of self-consistent relations is complemented by equations for $\langle n_{\mathrm{d}}\rangle$ and $\langle n_{\mathrm{f}}\rangle$, which are

$$\langle n_{\mathrm{d}}\rangle = T\sum_{\omega_n} G^{\mathrm{d}}_{ii}(\omega_n)\,\mathrm{e}^{\mathrm{i}\omega_n 0^+}, \tag{9}$$

and

$$\langle n_{\mathrm{f}}\rangle = \left\{1 + \exp\left[-(E_{\mathrm{f}} - \mu)/T + \sum_n L_n\,\mathrm{e}^{\mathrm{i}\omega_n 0^+}\right]\right\}^{-1}, \tag{10}$$

with

$$L_n \equiv \ln[\mathrm{i}\omega_n + \mu - \mathcal{A}(\omega_n)] - \ln[\mathrm{i}\omega_n - U + \mu - \mathcal{A}(\omega_n)], \tag{11}$$

the latter being obtained from the exact partition function [14]. For a given particle density n, and some definite relation between the two average occupation numbers, equations (9) and (10) determine the chemical potential μ and the energy E_{f}. For instance, in the paramagnetic case the occupation numbers satisfy the simple relationship $\langle n_{\mathrm{f}}\rangle = \langle n_{\mathrm{d}}\rangle = n/2$.

We now turn to the AF solution, still within the one-band model. We suppose that the lattice is bipartite, and divide it into a spin-up sub-lattice A and a spin-down sub-lattice B. The AF condition is

$$\langle n_{\mathrm{d}}\rangle_{\mathrm{A}} - \langle n_{\mathrm{f}}\rangle_{\mathrm{A}} = \langle n_{\mathrm{f}}\rangle_{\mathrm{B}} - \langle n_{\mathrm{d}}\rangle_{\mathrm{B}} = M, \tag{12}$$

where M stands for the sub-lattice magnetization. The local Green's function obtained from the effective one-site problem will keep its form, as given by (8), in each sub-lattice, i.e.,

$$G^{\mathrm{d}}_{ii\alpha}(\omega_n) = \frac{1 - \langle n_{\mathrm{f}}\rangle_\alpha}{\mathrm{i}\omega_n + \mu - \mathcal{A}_\alpha(\omega_n)} + \frac{\langle n_{\mathrm{f}}\rangle_\alpha}{\mathrm{i}\omega_n - U + \mu - \mathcal{A}_\alpha(\omega_n)}, \tag{13}$$

where $\alpha = A, B$. The self-consistency condition (7) now assumes the form [10]

$$G^{\mathrm{d}}_{ii\alpha}(\omega_n) = \frac{\xi}{\xi_\alpha}\int \frac{\rho_0(\varepsilon)}{\xi - \varepsilon}\,\mathrm{d}\varepsilon, \tag{14}$$

with

$$\xi_\alpha \equiv [G^{\mathrm{d}}_{ii\alpha}(\omega_n)]^{-1} + \mathcal{A}_\alpha(\omega_n), \qquad \xi \equiv \sqrt{\xi_{\mathrm{A}}\xi_{\mathrm{B}}}. \tag{15}$$

The average occupation numbers are obtained from generalizations of equations (9)–(11), with appropriate introduction of sub-lattice labels. We do not rewrite these equations here.

Since we have symmetry under spin reversal, we expect that μ and E_{f}, which fix the number of particles averaged over both sub-lattices, should remain the same as determined in the paramagnetic state. Thus, for each temperature, we first solve the paramagnetic problem with fixed occupation numbers of both particle species to determine μ and E_{f}; then, we solve the AF problem for fixed μ and E_{f} to determine the new occupation numbers, which yield the sub-lattice magnetization.

4. DMFT—the two-band problem

The procedure outlined in section 3 will now be extended to the two-band model defined by (2). The d-hole problem is treated similarly to what was done for a single band, except that the connection between different d orbitals occurs through an oxygen site. Thus, roughly speaking, the hopping integral is now replaced by a product of two d–p hoppings and a bare local p Green's function, $g_{\mathrm{p}}(\omega_n) = (\mathrm{i}\omega_n + \mu)^{-1}$.

As we mentioned before, we will use the DMFT as an approximation, without taking the infinite-dimension limit, but sticking to the specific two-dimensional geometry of the CuO_2 planes. Then, the d–p hybridization in $\mathbf{k}$ space can be written as $2t\gamma_{\mathbf{k}}$, where

$$\gamma^2_{\mathbf{k}} = 1 - \epsilon_{\mathbf{k}}, \qquad \epsilon_{\mathbf{k}} = \tfrac{1}{2}\sum_{\nu=1}^{2}\cos k_\nu. \tag{16}$$

We recognize in this last equality the tight-binding energies of a square lattice of unit lattice constant, normalized to dimensionless values in the range $-1 \leqslant \epsilon_{\mathbf{k}} \leqslant 1$.

In the paramagnetic state, the analogue of (4) is now

$$G^{\mathrm{d}}_{\mathbf{k}}(\omega_n) = \frac{1}{\mathrm{i}\omega_n + \Delta - 4t^2\gamma^2_{\mathbf{k}} g_{\mathrm{p}}(\omega_n) - \Sigma(\mathbf{k},\omega_n) + \mu}, \tag{17}$$

or, using (16),

$$G^{\mathrm{d}}_{\mathbf{k}}(\omega_n) = \frac{1}{\mathrm{i}\omega_n + \Delta - \Sigma(\omega_n) + \mu - 4t^2 g_{\mathrm{p}}(\omega_n)[1 - \epsilon_{\mathbf{k}}]}, \tag{18}$$

where we have already taken the self-energy as independent of wavevector. Likewise, the effective single-site Green's function, given by (5) in the one-band case, is now written as

$$G^{\mathrm{d}}_{ii}(\omega_n) = \frac{1}{\mathrm{i}\omega_n + \Delta - \Sigma(\omega_n) + \mu - 4t^2 g_{\mathrm{p}}(\omega_n) - \mathcal{A}(\omega_n)}, \tag{19}$$

with the resulting self-consistency condition

$$G^{\mathrm{d}}_{ii}(\omega_n) = \int \frac{\rho_0(\varepsilon)\,\mathrm{d}\varepsilon}{[G^{\mathrm{d}}_{ii}(\omega_n)]^{-1} + \mathcal{A}(\omega_n) - 4t^2 g_{\mathrm{p}}(\omega_n)\varepsilon}. \tag{20}$$

Explicit solution of the single-site problem gives $G^{\mathrm{d}}_{ii}(\omega_n)$ with the same form as in (8), except for the energy displacement Δ, and an extra term $-4t^2 g_{\mathrm{p}}(\omega_n)$ in both denominators.

It is, then, straightforward to generalize to the AF case. The single-site d-hole Green's function for each sub-lattice ($\alpha = \mathrm{A}, \mathrm{B}$) reproduces the form of (13), again with the addition of $\Delta - 4t^2 g_{\mathrm{p}}(\omega_n)$ to both denominators. We do not include spin polarization of the p levels, due to their low filling in the relevant low-doping regime. The self-consistency condition can be written as

$$G^{\mathrm{d}}_{ii\alpha}(\omega_n) = \frac{\tilde{\xi}}{\xi_\alpha} \int \frac{\rho_0(\varepsilon)}{\tilde{\xi} - \varepsilon}\,\mathrm{d}\varepsilon, \tag{21}$$

where we keep the definitions (15), i.e., $\xi_\alpha \equiv [G^{\mathrm{d}}_{ii\alpha}(\omega_n)]^{-1} + \mathcal{A}_\alpha(\omega_n)$, and additionally define

$$\tilde{\xi} \equiv \frac{\xi_{\mathrm{p}}\xi}{4t^2} = \frac{\xi_{\mathrm{p}}}{4t^2}\sqrt{\xi_{\mathrm{A}}\xi_{\mathrm{B}}}, \tag{22}$$

with $\xi_{\mathrm{p}} \equiv [g_{\mathrm{p}}(\omega_n)]^{-1} = \mathrm{i}\omega_n + \mu$. Again, we use the AF condition (12), and calculate the occupation numbers through generalizations of equations (9)–(11), where in the latter, besides the sub-lattice label, a term $\Delta - 4t^2 g_{\mathrm{p}}(\omega_n)$ is present in the arguments of both logarithms.

In contrast to the one-band problem, here we must take into account the occupation of p orbitals when fixing the total hole density to evaluate the chemical potential. The average number of p-holes per unit cell will have a contribution from the bare non-bonding p-orbital combination, and another one obtained by summing over wavevectors the full lattice Green's function of the hybridizing p levels, which can be written as

$$G^{\mathrm{p}}_{\mathbf{k}}(\omega_n) = \frac{1 + 2t^2\xi_{\mathrm{p}}^{-1}\left(\xi_{\mathrm{A}}^{-1} + \xi_{\mathrm{B}}^{-1}\right)}{\xi_{\mathrm{p}} - 4t^2\xi^{-1}\,\epsilon_{\mathbf{k}}}. \tag{23}$$

With the above set of self-consistent equations, we can study the electronic structure, i.e., the interacting DOS, as well as the sub-lattice magnetization, and the Néel temperature for a variety of model parameters. The interacting densities of states for each kind of particle are obtained from the imaginary parts of analytically continued Matubara Green's functions to real frequencies.

Before discussing these results, we want to stress that in the energy integrations we use the actual square-lattice bare DOS, given by

$$\rho_0(\varepsilon) = \frac{4}{\pi^2}\theta(1 - |\varepsilon|)\frac{1}{1 + |\varepsilon|}K\left(\frac{1 - |\varepsilon|}{1 + |\varepsilon|}\right), \tag{24}$$

in terms of the elliptical integral

$$K(k) = \int_{-\infty}^{\infty} \frac{\mathrm{d}x}{[(1 - x)(1 - k^2x^2)]^{1/2}}. \tag{25}$$

In the numerical calculations, we employ appropriate expansions of this elliptical integral, near its singular middle point or away from it.

5. Results

We are now ready to discuss numerical results obtained using the set of equations derived in section 4. Initially, we focus on the stability of AF ordering. We start with values of model

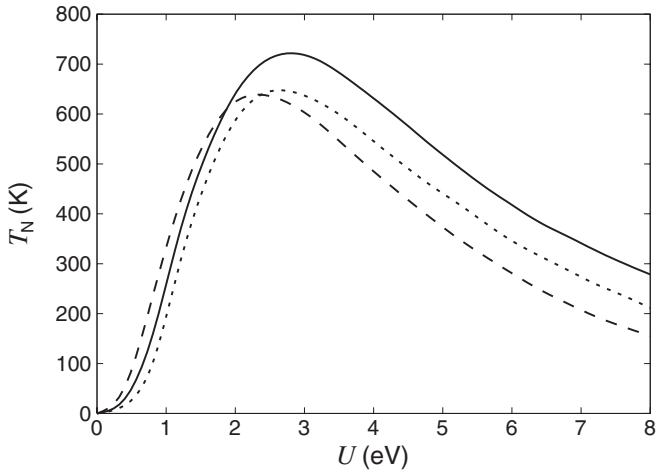

Figure 1. Variation of the Néel temperature with Coulomb correlation, under the condition $U = 2\Delta$, for three values of the hole density: $n = 1.0$ (full line), 0.9 (dashed), and 1.03 (dotted).

parameters in a range often used in the literature, choosing $t = 1$ eV, $U = 7.2t$, $\Delta = 3.6t$, so that $U = 2\Delta$. Then, for $n = 1$ (undoped case), we find an AF phase, i.e., a non-zero sub-lattice magnetization that survives up to a Néel temperature of ∼325 K, in reasonable agreement with experimental observations in cuprates [20].

In order to further explore the model and method, we studied T_N as a function of the Coulomb interaction U, for a few values of hole concentrations around $n = 1$, keeping the condition $U = 2\Delta$. Our results, plotted in figure 1, show a maximum Néel temperature for $n = 1$ and $U \simeq 2.8t$. This value of U, and the corresponding Δ, are substantially smaller than usually taken as appropriate to the known HTSC compounds. It is interesting to notice that the T_N curves of figure 1 correctly interpolate between the strong-coupling regime, where a Heisenberg-like behaviour is reproduced, and the weak-coupling limit, where T_N vanishes for vanishing U and Δ.

We generalized our study still further, by allowing both U and Δ to vary independently. Figure 2 shows a three-dimensional plot of the Néel temperature as a function of both parameters, for $n = 1$. We can see the line $U = 2\Delta$ passes near the absolute maximum, although it is nearly perpendicular to the 'ridge' line of T_N maxima. Then, for simplicity, we fix the relationship $U = 2\Delta$ in order to study the doping dependence of T_N.

By varying the number of holes, we were able to construct the phase diagrams shown in figure 3, both for the usual $U = 7.2t$ and for the optimum value $U = 2.8t$. We obtain that T_N is highest for the undoped case ($n = 1$), as expected. It can be seen that for $U/t = 7.2$ the AF solution is stable within a narrow range around $n = 1$, in good agreement with experimental observations. For $U/t = 2.8$, the AF phase is more robust, with higher Néel temperatures, reaching a maximum of approximately 720 K for $n = 1$, and presenting an enlarged stability region against doping. A small asymmetry is observed with respect to doping by holes ($n > 1$) or electrons ($n < 1$). This kind of asymmetry is present in real systems, but a direct comparison is not possible, as these two regions refer to different compounds, implying that to be realistic we should use different parameter values on each side of the phase diagram.

We want to mention that a phase diagram bearing similar features to ours was obtained by Maier *et al* [21], for nearly the same parameters as used for the inner curve of figure 3. They also used a DMFT approach, but solved the local problem via NCA. An important difference

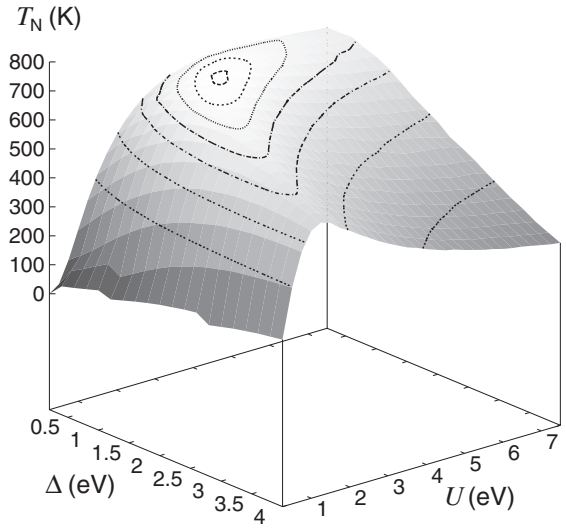

Figure 2. Variation of the Néel temperature with Coulomb correlation and charge-transfer gap in the undoped case.

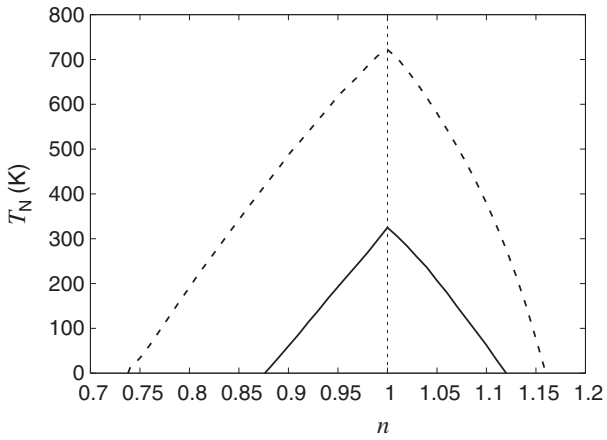

Figure 3. Phase diagram showing T_N as a function of the hole concentration n, for $U = 7.2t$ (full line) and $U = 2.8t$ (dashed). In both cases the condition $\Delta = U/2$ holds.

between those results and ours is that they find a *displaced* phase diagram, with the maximum T_N occurring slightly above $n = 1$. The authors argue that their choice of parameters induces a shift of the metal–insulator transition towards higher hole doping. We believe that this is actually an artifact of their approximation (NCA). Displacement of the transition was also obtained [9] with an extended Hubbard I approximation, and reflects a spurious shift of spectral weight to the lowest lying bands. Here, we always obtain the maximum Néel temperature and the metal–insulator transition at zero doping ($n = 1$), as can be seen for both cases shown in figure 3.

We now turn to the one-particle densities of states. We will concentrate on the largest-T_N case, $U = 2\Delta = 2.8t$, although the qualitative picture is reproduced for other parameter

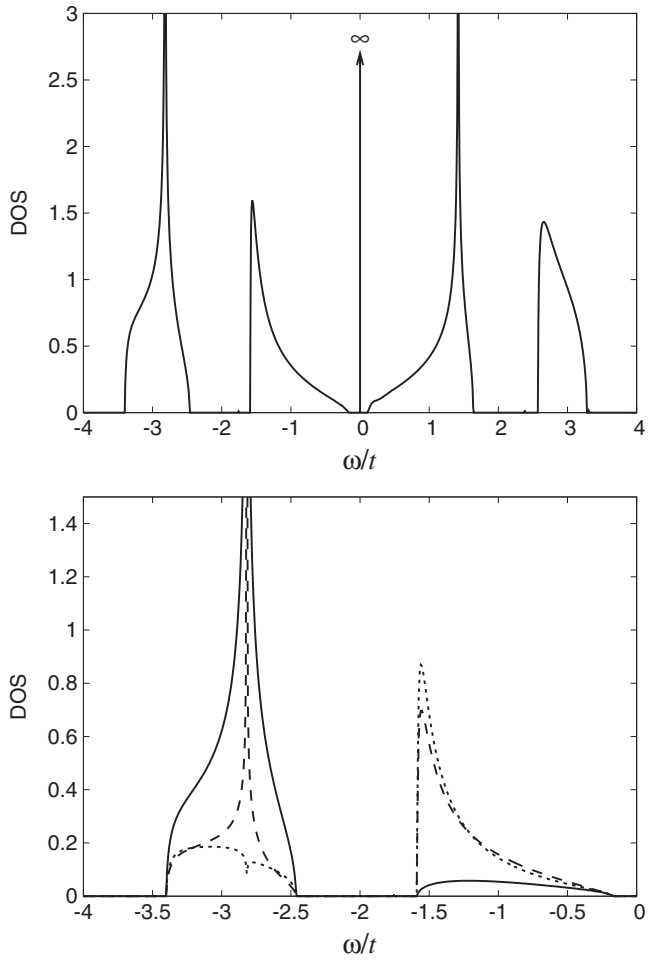

Figure 4. DOS in the AF case, for $U = 2.8t$, $\Delta = U/2$, $n = 1$, and $T \to 0$. Top panel: full-range total DOS, including the non-bonding p-band at $\omega = 0$. Bottom panel: low-energy sector, explicitly showing all contributions: up-spin d (full line), down-spin d (dotted line), and p (dashed line).

values, provided we remain in the charge-transfer case $U > \Delta$. The DOS for $n = 1$ and $T \to 0$ is shown in figure 4, with a full-range plot of the total DOS in part (a), and a more detailed view of the low-energy sector in part (b). The chemical potential falls inside the first (charge-transfer) gap. We can see that the bands are all hybrid (mixed d and p), and strongly spin polarized. It is important to emphasize that the effective charge-transfer gap observed in figure 4 is lower than Δ, which is an excitonic effect predicted in the early days of HTSC [22], and can be related to the so called Zhang–Rice singlet [6]. Also noticeable are the sharp peaks due to the logarithmic van Hove singularities of $\rho_0(\varepsilon)$. As the temperature is increased (not shown in the figure), we observe a rounding off of these peaks, together with a reduction of the spin polarization, which completely disappears at T_N. The effect of doping (at fixed temperature) is also to reduce the spin polarization as the AF stability limit is approached, while the inter-band gaps are narrowed, and the chemical potential moves into one of the bands at either side of the gap, depending on whether the system is doped with electrons or holes.

The low-energy behaviour is very similar to what would happen in a single-band model, which in part supports the generally accepted assertion that the relevant physics of HTSC can be obtained from a Hubbard model near half-filling, with a properly chosen effective on-site repulsion U^{eff}. We can see that this effective repulsion is more closely related to the charge-transfer gap than with the Coulomb interaction itself. On the other hand, we wish to point out that, in contrast to a half-filled single-band system, the actual lowest-lying bands are *not* symmetrical, with a larger spectral weight concentrated in the occupied band. This is due to the fact that we have hybridization between a nearly half-filled (strongly correlated) band and an almost empty (uncorrelated) one. This constitutes an important distinction between the low-energy physics of HTSC as described by the three-band and the single-band Hubbard models.

6. Conclusions

In this paper, we have used the DMFT approach to study the magnetic phase diagram and DOS of a simplified three-band Hubbard model, in which particles with a given spin orientation have their dynamics frozen when evaluating spectral properties of particles with the opposite spin orientation. Studying the stability of magnetic ordering against doping, in the strong-correlation limit, and for fairly large charge-transfer gap, we were able to obtain values of the Néel temperature in a range consistent with experimental observations for HTSC cuprates, as well as good qualitative agreement for the behaviour of T_{N} as a function of doping.

In order to access the model's potentialities, we left the experimental region of coupling constants, and freely explored the parameter space, more specifically, varying the charge-transfer gap and the Coulomb correlation. We then showed that T_{N} can be substantially enhanced by reducing the correlation strength while remaining within the charge-transfer-insulating regime ($U > \Delta$). These results suggest that less strongly correlated systems, with smaller charge-transfer gaps as compared to the HTSC cuprates, if experimentally realizable, should show higher Néel temperatures.

Unfortunately, within the present approach it is not possible to infer what would happen with the superconducting critical temperature T_{c} upon the same variation of parameters. If there is some correlation between the values of T_{N} and T_{c}, such that T_{c} rises in the superconducting regime (higher doping) when T_{N} rises in the magnetic one, we could also expect higher temperatures for the superconducting solution.

Finally, based on our analysis of the one-particle densities of states, we wish to stress the fact that, even though the low-energy physics is dominated by two (sub)bands separated by a gap, the nature of these bands and, in particular, their spectral-weight asymmetry raise doubts about the soundness of a simple mapping into an effective one-band Hubbard model.

Acknowledgment

We acknowledge support from Conselho Nacional de Desenvolvimento Científico e Tecnológico (CNPq), Brazil.

References

[1] Bednorz J G and Müller K A 1986 *Z. Phys.* B **64** 189
[2] Bardeen J, Cooper L N and Schrieffer J R 1957 *Phys. Rev. Lett.* **106** 162
Bardeen J, Cooper L N and Schrieffer J R 1957 *Phys. Rev. Lett.* **108** 1175
[3] Damascelli A, Hussain Z and Shen Z-X 2003 *Rev. Mod. Phys.* **75** 473

[4] Khasanov R, Schneider T, Brütsch R, Gavillet D, Karpinski J and Kelleret H 2004 *Phys. Rev.* B **70** 144515
[5] Pimenov A, Loidl A, Jakob G and Adrian H 2000 *Phys. Rev.* B **61** 7039
[6] Zhang F C and Rice T M 1988 *Phys. Rev.* B **37** R3759
[7] Emery V J 1987 *Phys. Rev. Lett.* **58** 2794
[8] Hubbard J 1963 *Proc. R. Soc.* A **276** 238
[9] Beatrici A and Gusmão M A 1995 *Phys. Rev.* B **51** 7508
[10] Georges A, Kotliar G, Krauth W and Rozemberg M J 1996 *Rev. Mod. Phys.* **68** 13
[11] Metzner W and Vollhardt D 1989 *Phys. Rev. Lett.* **62** 324
[12] van Dongen P G J and Vollhardt D 1990 *Phys. Rev. Lett.* **65** 1663
[13] Falicov L M and Kimball J C 1969 *Phys. Rev. Lett.* **22** 997
[14] Brand U and Mielsch C 1989 *Z. Phys.* B **75** 365
Brand U and Mielsch C 1990 *Z. Phys.* B **79** 295
[15] Freericks J K and Zlatić V 2003 *Rev. Mod. Phys.* **75** 1333
[16] Consiglio R and Gusmão M A 1997 *Phys. Rev.* B **55** 6825
[17] Craco L and Gusmão M A 1996 *Phys. Rev.* B **54** 1629
[18] Brinckman J and Greene N 1981 *Z. Phys.* B **84** 179
[19] Letz M and Gooding R J 1998 *J. Phys.: Condens. Matter* **10** 6931
[20] Demler E, Hanke W and Zhang S-C 2004 *Rev. Mod. Phys.* **76** 909
[21] Maier Th, Zölfl M B, Pruschke Th and Keller J 1999 *Eur. Phys. J.* B **7** 377
[22] Varma C M, Schmitt-Rink S and Abrahams E 1987 *Solid State Commun.* **62** 681